Science Advances AAAS

Argon constraints on the early growth of felsic continental crust

Meng Guo[1*], Jun Korenaga[1]

[1]Department of Geology and Geophysics, Yale University, New Haven, CT, USA.

*Correspondence: meng.guo@yale.edu

Abstract

The continental crust is a major geochemical reservoir, the evolution of which has shaped the surface environment of Earth. In this study, we present a new model of coupled crust-mantle-atmosphere evolution to constrain the growth of continental crust with atmospheric $^{40}Ar/^{36}Ar$. Our model is the first to combine argon degassing with the thermal evolution of Earth in a self-consistent manner and to incorporate the effect of crustal recycling and reworking using the distributions of crustal formation and surface ages. Our results suggest that the history of argon degassing favors rapid crustal growth during the early Earth. The mass of continental crust, highly enriched in potassium, is estimated to have already reached >80% of the present-day level during the early Archean. The presence of such potassium-rich, likely felsic, crust has important implications for tectonics, surface environment, and the regime of mantle convection in the early Earth.

One sentence summary: The degassing history of argon favors the rapid growth of felsic continental crust in the early Earth.

MAIN TEXT

Introduction

The continental crust covers ~40 % of Earth's surface and accounts for ~80 % of the total volume of Earth's crust. Its relatively low density and great thickness allow its surface to be exposed above sea level, providing a unique environment for life. The evolution of continental crust is directly linked with a number of important issues in Earth sciences, such as the origin of plate tectonics (*1*), the history of mantle degassing (*2*), and the distribution of heat producing elements within the solid Earth (*3*). During crustal formation, incompatible elements in the parental mantle, which include rare earth elements and heat-producing elements such as K, U, and Th, are preferentially partitioned to the crust, and noble gases are degassed to the atmosphere. In addition, crustal recycling continuously returns incompatible elements to the mantle, and along with crustal reworking, they redistribute these elements among silicate reservoirs. Consequently, even though the continental crust comprises only ~0.5 % of the mass of the bulk silicate Earth, it is a major geochemical reservoir, whose composition places significant constraints on the chemical budget of other terrestrial reservoirs. Thus, understanding how the mass of continental crust and its composition evolve helps unravel the workings of the Earth system as a whole.

A number of Earth scientists have tried to constrain crust-mantle evolution (e.g., *4-8*). Whereas the existing models of continental growth exhibit great diversity, it has recently been shown that such diversity is mostly superficial (*9*). Following the classification scheme of Korenaga (*9*), we can group them into three categories: crust-based, mantle-based, and others. Crust-based models are estimates on the present-day distribution of the formation age of continental crust (e.g., *5*, *10*, *11*). They do not contain information of the crust that has been recycled into the mantle, thereby serving as the lower bound on net crustal growth. Mantle-based models aim at the net growth of continental crust, by utilizing the complementary nature of the depleted mantle and the crust (e.g., *7*, *8*). Because of crustal recycling, the appearance of these two types of models can be very different, but this does not necessarily indicate inconsistency. In fact, the latest crust-based model (*11*) and the latest mantle-based model (*8*) are in agreement with each other, once the effect of recycling is taken into account.

In this study, we aim to constrain continental evolution using the history of argon degassing. This approach belongs to the third category of crustal growth models (e.g., *2*, *12*), because it aims at net growth of continental crust using less direct, albeit quantitative, constraints than the mantle-based approach. Nevertheless, using the degassing history of Earth allows us to understand crustal growth in the broader framework of the Earth system. Inert noble gases residing in the atmosphere are an integrated result of degassing from the Earth's interior, and as such, they can potentially provide important insights into the evolution of terrestrial reservoirs (e.g., *13*). The relation between crustal growth and argon degassing has been explored most recently by Pujol et al. (*2*); they provided estimates on the $^{40}Ar/^{36}Ar$ of the Archean atmosphere derived from measurements of Archean hydrothermal quartz and used the box model of Hamano and Ozima (*14*) to infer crustal growth. Given the possibility of radiogenic ^{40}Ar added from the sample, the estimates provided by Pujol et al. (*2*) are better to be seen as an upper bound on the $^{40}Ar/^{36}Ar$ of the Archean atmosphere. Even with this limitation, their estimates still present a new exciting opportunity for this field, because degassing models have long suffered from the lack of observational constraints on the ancient atmosphere.

However, as in a number of previous studies, Pujol et al. (*2*) used directly the net growth of continental crust in their model. Such simplistic treatment of continental growth does not acknowledge that net growth is a product of a dynamic balance between new crust generation and crustal recycling, and as a result, the effect of crustal growth on argon degassing is severely underestimated in their study. Also, the other aspects of their model, such as the timing of sudden degassing and the mode of thermal evolution, are difficult to justify. For example, a sudden degassing event, which plays an important role in the early phase of argon degassing, represents the collective effect of giant impacts, and its timing corresponds to the Moon-forming giant impact. While the details of giant impacts remain debated, all of the solutions of Pujol et al. (*2*) begin with an atmospheric $^{40}Ar/^{36}Ar$ of 50 at 170 Myr after the beginning of solar system. With an earlier timing of the last giant impact, which is more consistent with recent estimates on the age of the Moon (e.g., *15*), the sudden degassing event cannot effectively elevate the atmospheric $^{40}Ar/^{36}Ar$ as high as 50. Similarly, their assumption on the history of mantle degassing, which is inherited from the model of Hamano and Ozima (*14*), is grossly outdated, given the recent development on the thermal evolution of Earth (e.g., *1*, *9*).

In light of the above, we have built a more comprehensive model of argon degassing to better understand its constraints on crustal growth. Our model is the first to investigate the full effects of crustal evolution, including both crustal recycling and reworking, on the degassing history of Earth. Here, the term 'crustal recycling' is used to denote the loss of continental crust to the mantle through subduction and delamination, whereas the term 'crustal reworking' refer to the processes that change isotopic compositions and reset the apparent age of the preexisting crust (e.g., erosion, sedimentation, and partial melting). Crustal recycling affects both the continental crust and the mantle, while crustal reworking takes place within the continental crust. Also, the net growth of continental crust is defined to be the evolution of continental mass present on the Earth's surface, i.e., with the effect of crustal recycling already taken into account. Our model also incorporates geophysical and geochemical constraints on the thermal evolution of Earth and utilizes several robust geological observations to depict a coherent story of continental evolution. Most previous crustal growth models are based on one kind of observation from either geochemical, geophysical, or petrological aspect. However, these observations provide different and complementary constraints on crust formation. In our new model, we use the $^{40}Ar/^{36}Ar$ of the present-day atmosphere (*16*) as well as the Archean atmosphere (*2*) to constrain argon degassing, the distributions of formation age (*11*) and surface age (*17*) of continental crust to constrain the extent of crustal recycling and reworking, and Archean and Proterozoic mantle potential temperatures (*18*) to constrain the thermal history of Earth. In what follows, we first present a brief description of our modeling strategy, then summarize model results, and discuss how the history of argon degassing constrains crustal evolution. The details of our box modeling are given in the Methods section.

Model Formulation and Results

We have built a box model to simulate the degassing history of argon, using the following three terrestrial reservoirs: the mantle, the continental crust, and the atmosphere. As in traditional degassing models, the oceanic crust is not considered as a major reservoir in our model because of its relatively short residence time. However, degassing caused by oceanic crust formation is tracked throughout Earth history and is part of the total rate of mantle degassing. Among the three reservoirs, the mantle degasses argon into the atmosphere through magmatism, and the crust does so through crustal recycling and reworking. Potassium-40, which decays to argon-40, is transferred to the continental crust from the mantle during partial melting, and part of it is recycled back into the mantle through subduction. To understand how the model is constrained by different observations, we conduct our modeling in three stages, first with crustal evolution only, then with thermal evolution, and finally with the history of argon degassing. We choose to use simple Monte Carlo sampling for all three stages of our modeling. By comparing the a posteriori distributions of model parameters with their a priori distribution, this simple random sampling allows us to better quantify how each stage constrains crustal evolution. A total of 16 independent variables (Table 1) are used to control the details of these three stages, and 6 dependent variables (Table 2) are used to ensure internal consistency between the thermal and chemical evolution of Earth. Following Rosas and Korenaga (*8*), crustal evolution is parameterized using the onset of crustal growth (t_s), the initial and present-day crustal recycling rates (R_s and R_p), and the decay constants of crustal recycling and growth rates (κ_r and κ_g). The extent of crustal reworking is controlled by the reworking factor (f_{rw}), which is the fraction of the initial reworking rate with respect to the initial recycling rate. A wide range of crustal evolution can be modeled by varying these six parameters, and it is relatively easy to find various combinations of those parameters that can satisfy the observed crustal formation and surface age distributions. Even with simple Monte Carlo sampling, the sampling efficiency is about 10 %. Next, we couple the accepted models of crustal evolution with different models for the thermal evolution of Earth, by taking into account the uncertainties of heat productions and heat fluxes of terrestrial reservoirs. Because these uncertainties are relatively small, it is also easy to find adequate thermal budgets to satisfy the history of mantle cooling during the Archean and Proterozoic; the sampling efficiency at the second stage is as high as about 50 %. Lastly, we couple the successful combinations of crustal evolution and thermal evolution with different scenarios of argon degassing, by testing the impact of early sudden degassing as well as incomplete degassing during mantle magmatism. Successful solutions at the third stage are chosen on the basis of the argon isotopic abundances of the present-day atmosphere and $^{40}Ar/^{36}Ar$ in the Archean atmosphere. This stage is most time-consuming, and from 8 x 10^6

iterations of Monte Carlo sampling, we have collected a total of ~3 x 10^3 successful solutions that exhibit good agreements with all of the observational constraints (Fig. 1).

The a posteriori distributions of the parameters R_s, R_p, t_s, κ_r, κ_g, and f_{rw} characterize important features of crustal evolution models selected at different stages (Fig. 2). Based on our previous work (*8*), R_s and R_p have a priori ranges of 0 to 10 × 10^{22} kg Gyr^{-1} and 0 to 2 × 10^{22} kg Gyr^{-1}, respectively, and κ_r is varied from -3 to 3 Gyr^{-1} to cover from convex to concave evolution patterns for crustal recycling, whereas κ_g is varied from -1 to 30 Gyr^{-1} to cover from late-stage to instantaneous crustal growth. The onset time t_s is varied from 0.057 to 0.567 Gyr, i.e., from the likely timing of the Moon-forming giant impact (*15*) to the end of Hadean. The temporal evolution of crustal reworking is assumed to follow that of crustal recycling, and different reworking rates are tested by varying f_{rw} within the range of 0.1 to 0.8. Compared to stage three, stages one and two do not provide tight constraints on crustal evolution; most parameters exhibit nearly uniform distributions (Figs. 2D to 2F), with a slight preference to low recycling rates (Figs. 2A to 2C). However, all successful solutions at stage three have R_s larger than 2.5 × 10^{22} kg Gyr^{-1} (Fig. 2A), R_p smaller than 9.5 × 10^{21} kg Gyr^{-1} (Fig. 2B), and κ_r larger than 0.2 Gyr^{-1} (Fig. 2C), favoring crustal evolution with intense recycling at the beginning followed by rapid decrease. The rate of crustal reworking is similarly high as that of crustal recycling, as indicated by the distribution of f_{rw} (Fig. 2F). Both recycling and reworking are responsible for vigorous crustal degassing in the early Earth, and consequently, the rise of atmospheric $^{40}Ar/^{36}Ar$ in the Archean (Fig. 1A). Net crustal growth models are characterized by κ_g, and ~80% of the successful solutions have κ_g larger than 3 Gyr^{-1}, i.e., rapid crustal growth in the early Earth (Fig. 2D). Such rapid crustal generation contributes to elevating the atmospheric $^{40}Ar/^{36}Ar$ to ~100 at the beginning of the Archean, which is important for matching the Archean constraints (Fig. 1A). The distribution of t_s is rather uniform with some preference to later onset (Fig. 2E), which gives time for ^{40}K to decay and stock terrestrial inventories of ^{40}Ar. The evident contrast between the distributions from stage three and those from previous stages indicates that degassing history is sensitive to different models of crustal formation and thus can place useful constraints on continental growth. For the a posteriori distributions of other model parameters, see Fig. S1.

The preferred models of crustal evolution, as determined by the parameters mentioned above, are visualized in Fig. 3. About 80% of the net crustal growth display rapid formation during the early Archean, with the crustal mass being comparable to the present-day value (Fig. 3A). Such early formation challenges the popular notion of less than 30% of continental crust in the Archean (*2*, *7*, *12*), but it is essential to match the atmospheric $^{40}Ar/^{36}Ar$ in the Archean (Fig. 1A). All successful solutions exhibit high crustal generation during the early Earth, which requires vigorous mantle melting and results in significant mantle degassing (Fig. 3B). The rapid crustal growth generates a substantial amount of Hadean and Archean continental crust, but as constrained by the distributions of crustal formation and surface ages, intense early recycling and reworking are also necessary to erase and reset the records of the old crust (Figs. 3C & 3D), with only ~1 % and ~10 %, respectively, preserved at present-day from the Hadean and early Archean (Figs. 1C & 1D). As a consequence, vigorous crustal degassing during the early Archean is achieved through recycling and reworking, and along with mantle degassing, they have elevated the atmospheric $^{40}Ar/^{36}Ar$ (Fig. 1A).

In order to understand how different degassing processes contribute to the atmospheric argon abundance, their instantaneous and cumulative contributions are compared in Fig. 4. In our model, the modern degassing rate of ^{40}Ar from the solid Earth ranges from 7.1×10^7 to 3.6×10^8 mol/yr, which is broadly consistent with the estimate of Bender et al. (*19*) ($1.1 \pm 0.1 \times 10^8$ mol/yr).

It is noted that our model can reproduce an acceptable present-day degassing rate, without using such a constraint. The mantle degasses argon at different rates while generating continental crust (K_{mc}), oceanic crust (K_{mo}), and hotspot islands (K_{mp}). Among them, K_{mc} is calculated from the rate of crustal generation, with the consideration of continental crust being the secondary product of oceanic crust (Equations 4 and 5), while K_{mo} and K_{mp} are inferred from the thermal history of the Earth, with the possibility of incomplete degassing taken into consideration (Table 2). With K_{mc} being the largest contributor to the atmospheric ^{40}Ar through Earth history (Fig. 4A), approximately 50% of the present-day abundance originates in the generation of continental crust (Fig. 4B), which demonstrates that continental growth greatly affects the degassing history of Earth. The continental crust can release a significant amount of ^{40}Ar in the early Archean through recycling (K_{rc}) and reworking (K_{rw}) (Fig. 4A), thanks to abundant parent isotope ^{40}K in the crust. Whereas the major element composition of continental crust is not directly considered in our modeling, the crust that is as enriched in potassium as the present-day crust should be closer to felsic than mafic. A large quantity of such felsic-like crust in the early Earth (e.g., *20*) conflicts with the prevailing notion of little felsic crust in the early Archean (e.g., *3*, *12*, *21*), requiring a careful rethinking of tectonics, surface environment, and the style of mantle convection during the early Earth.

Discussion

Our results show that the degassing history of argon is sufficiently sensitive to different modes of net crustal growth, and all of our successful solutions are consistently characterized by rapid crustal generation with intense recycling and reworking during the early Earth (Fig. 3). The preference for such rapid crustal evolution is largely guided by the high ^{40}Ar/^{36}Ar of the Archean atmosphere. In our model, the potassium content in the continental crust is first tracked backward in time using its decay constant and present-day concentration, and then scaled to be proportional to the growth of continental crust. As a consequence, the early crust is assumed to be as enriched in potassium as the present-day crust. The considerable contribution of crustal degassing to the Archean atmospheric ^{40}Ar (Fig. 4) indicates that such a large amount of potassium-enriched, thus possibly felsic crust during the early Earth was essential. The substantial amount of potassium-enriched crust does not necessarily indicate that the continental crust like today already existed in early Archean, but the equivalent amount of potassium in the crust is required to explain the atmospheric ^{40}Ar. In other words, our model constrains the evolution of crustal mass based on the assumption that the crust is as enriched in potassium as the present-day crust through Earth history; if the early continental crust is not as felsic as assumed (e.g., *3*), our estimate on net crustal growth should serve as a lower bound. Because early crustal growth is already very rapid in our model, however, we suspect that the true crustal growth would not significantly deviate from this lower bound. The secular evolution of crustal composition has been studied with a variety of approaches using the geochemistry of sedimentary and igneous rocks, the weighted average of stratigraphic successions, crustal xenoliths, and seismic crustal structure (e.g., *3*, *22*, *23*, *24*), but the composition of early continental crust still remains controversial (e.g., *12*, *20, 21*). Our study provides a new constraint from a different perspective.

One important feature of our model is the simultaneous application of multiple observational constraints to ensure the internal consistency among the thermal evolution, crustal evolution, and degassing history of Earth, which also allows us to quantitatively investigate the effects of recycling and reworking on crustal degassing. This feature is one of the important differences between this study and Pujol et al. (*2*). Instead of mechanistically relating various crust-mantle differentiation processes with mantle degassing, Pujol et al. (*2*) modeled mantle degassing in an abstract manner, with only one parameter. As one can see from Fig. 4, however, the mantle degasses argon through three types of magmatism, each of which follows a different evolutionary trend. To make matters worse, their modeling of mantle degassing assumes an exponential decrease in the vigor of mantle convection. Recent progress on the thermal evolution of Earth, however, suggests more sluggish mantle convection in the past (e.g., *1*, *9*). Moreover, Pujol et al. (*2*) adopted the approach of Hamano and Ozima (*14*) to model the rate of crustal degassing, which was inferred from the difference between K-Ar mineral ages and Rb-Sr whole rock ages, i.e., they only considered the contribution of reworking to crustal degassing. Without taking into account the effect of crustal recycling, the total crustal contribution to degassing history is underestimated (Fig. 4). With such low crustal degassing, Pujol et al. (*2*) were able to match the Archean atmospheric constraint only by introducing a late onset of sudden degassing, which effectively elevated their atmospheric $^{40}Ar/^{36}Ar$ to 50 (see their Fig. 2a). As mentioned in the Introduction section, sudden degassing at 170 Myr is probably too late to be consistent with what geochronological studies suggest (e.g., *15*). Pujol et al. (*2*) provided an invaluable observational constraint on the ancient atmosphere, but for the aforementioned reasons, we reached different conclusions using the same Archean data.

The significant differences between Pujol et al. (*2*) and this study underline the importance of treating crustal evolution properly in degassing models, though this issue is not widely appreciated. For example, a recent study of mantle xenon isotopes (*25*) suggests that the deep volatile cycles shifted from a net degassing to a net regassing regime around 2.5 Ga. They used, however, the net growth of continental crust to calculate the mantle degassing rate corresponding to continental growth, which is the same treatment used by Pujol et al. (*2*). In fact, a recent study on Archean komatiites (*26*) suggests that the subduction of water was initiated before 3.3 billion years ago, which is more consistent with our modeling results. For these reasons, the degassing models that do not fully acknowledge the effect of continental growth (e.g., *25*, *27*) deserve to be revisited carefully.

As mentioned in the Introduction section, our model of crustal growth belongs to the third category, because it is inferred indirectly from the degassing history of Earth. Nevertheless, this model is in good agreement with the recent mantle-based model by Rosas and Korenaga (*8*), thereby reinforcing the notion of rapid crustal growth during the Hadean and the early Archean (Fig. 3A and their Fig. 1c). Based on the samarium-neodymium isotope systems, Rosas and Korenaga (*8*) were able to place a tighter bond on crustal evolution because the mantle-based approach is more direct. Given that potassium is much more incompatible than samarium and neodymium, however, our model can better constrain the compositional evolution of continental crust. Also, as a heavy noble gas, the atmospheric argon keeps an integrated degassing history of the bulk Earth, thus suffering less from preservation issues than mantle-based models, which rely critically on preserved rock samples. Crust-based models are essentially the present-day distribution of crustal formation ages, and with consideration of crustal recycling, both our study and Rosas and Korenaga (*8*) are in good agreement with the recent crust-based model of Korenaga (*11*), so the different approaches appear to be converging. The large offset between the rapid crustal growth (Fig. 3A) and the nearly linear distribution of formation ages (Fig. 1C) can be explained by a time-integrated effect of crustal recycling (*8*). This model of crustal evolution, characterized with rapid crustal growth and efficient crustal recycling in the early Earth, resembles closely what Armstrong suggested almost forty years ago (*28*).

The net growth of continental crust is controlled by a dynamic balance between crustal generation and recycling. The approximately zero net crustal growth after the Hadean, but with non-zero crustal recycling, indicates that new crust must have been continuously formed at the same rate of recycling (Fig. 3). Such persistent crustal formation and destruction through Earth history is consistent with the onset of plate tectonics in the very early Earth (e.g., *29*). Here, the term 'plate tectonics' is defined in a board sense, a mode of mantle convection with the continuous, wholesale recycling of surface layer, as opposed to stagnant lid convection. Our result of rapid crustal growth with efficient early recycling suggests vigorous mantle convection in the early Hadean, followed by a gradual decrease to the present-day level. Such decline in crustal generation may be explained by the secular cooling of the mantle (*18*), because a cooler mantle yields less voluminous melting. The corresponding decrease in crustal recycling may be attributed to an increasing preservation potential of continental crust (*9*). The positive net water flux from the surface into the mantle, as inferred from deep water cycle and continental freeboard (*30*), suggests the gradual hydration of the convecting mantle through time, and as a consequence, the continental mantle lithosphere, which remains dry owing to its generation mechanism, becomes stronger with respect to the convecting mantle, making crustal recycling less efficient (*1*). The mode of mantle convection in the early Earth is still controversial (e.g., *17*, *21, 29*), and more careful geodynamical work is warranted (*31*) to discuss whether mantle convection had switched from a different mode to modern plate tectonics under early Earth conditions.

Methods

As briefly described in the Model Formulation and Results section, the terrestrial reservoirs considered in our box model are the mantle, the continental crust, and the atmosphere. The mantle degases argon to the atmosphere through mantle magmatism, and the crust does so through crustal recycling and reworking. The potassium is transferred between the mantle and crust during partial melting and subduction. We modeled the crustal evolution first to constrain the mass transfer rates between mantle and crust, then simulated the thermal evolution of Earth to infer the rates of mantle magmatism, and calculated the degassing history of argon using the degassing rates acquired from the above two stages. The model formulation for each stage is described in details below.

Continental crust growth

As mentioned in the Model Formulation and Results section, we follow Rosas and Korenaga (*8*) for the parameterization of crustal growth and recycling rates:

$$M_{cc}(t) = \frac{M_{cc}(t_p)}{1-e^{-\kappa_g(t_p-t_s)}}\left(1 - e^{-\kappa_g(t-t_s)}\right), \ (1)$$

$$K_{rc}(t) = R_s + \frac{R_p-R_s}{1-e^{-\kappa_r(t_p-t_s)}}\left(1 - e^{-\kappa_r(t-t_s)}\right), \ (2)$$

$$\frac{dM_{cc}(t)}{dt} = K_{cc}(t) - K_{rc}(t), \ (3)$$

where $M_{cc}(t)$ is the mass of continental crust at time t. As shown in equation (3), the time derivative of $M_{cc}(t)$ equals to the difference between the crustal generation rate, $K_{cc}(t)$, and the crustal recycling rate, $K_{rc}(t)$. The present-day crustal mass $M_{cc}(t_p)$ is set to be 2.09 x10^{22} kg. The term t_s denotes the onset of crustal generation and recycling; R_s and R_p are the rates of crustal recycling at t_s and t_p, respectively; and κ_g and κ_r are the decay constants for K_{cc} and K_{rc}, respectively. A wide variety of crustal growth patterns can be tested in our model by varying these parameters, covering from late growth to nearly instantaneous growth.

The crustal generation rate $K_{cc}(t)$ describes how much mass has been added to the crust with time. To calculate the mantle processing rate corresponding to the generation of continental crust, $K_{mc}^{prod}(t)$, we use the complementary nature between the crust and the mantle:

$$K_{mc}^{prod}(t) = \frac{\frac{K_{cc}(t) N_{^{40}K}^{CC}(t)}{M_{cc}(t)}}{\frac{M_M(t)}{N_{^{40}K}^{M}(t)}}, \quad (4)$$

where $M_M(t)$ is the mass of the mantle at time t, and $N_{^{40}K}^{M}(t)$ is the number of ^{40}K atoms in the mantle at time t. Both of them can be inferred from mass balance among the mantle, the continental crust, and the bulk silicate Earth.

However, the continental crust does not result from the single-stage melting of the mantle. Considering that at least part of continental crust is likely to be produced through the secondary melting of oceanic crust, treating all of $K_{mc}^{prod}(t)$ as the mantle processed rate to generate continental crust can overestimate the total mantle processing rate. Following Padhi et al. (*32*), therefore, the mantle processing rate solely responsible for the generation of continental crust, K_{mc}, is calculated as follows:

$$K_{mc}(t) = \max\,(K_{mc}^{prod}(\mathrm{t}) - K_{mo}(t), 0). \quad (5)$$

Crustal reworking is likely to be in sync with recycling, as the former is necessary to break down the crust into subductable sediments, so we set the secular evolution of reworking to be similar to that of recycling, with a factor of f_{rw}, which varies between 0.1 to 0.8 in our model. The crustal reworking rate is therefore calculated as:

$$K_{rw}(t) = K_{rc}(t) f_{rw}. \quad (6)$$

Taking into account that reworking is responsible for the difference between the distributions of crustal formation and surface ages (*11*), we choose the acceptable reworking factor f_{rw} by calculating these distributions and comparing to observational constraints. To do so, we first follow Rosas and Korenaga (*8*) to model the formation age distribution of continental crust,

$m(t,\tau)$, where t is the time and τ represents the formation age. The summation of the $m(t,\tau)$ over time τ gives the total crustal mass at time t:

$$M_{CC}(t) = \int_0^t m(t,\tau)d\tau. \quad (7)$$

In our model, the continental crust is considered to be a homogeneous reservoir at all time, so recycling uniformly affects the crustal parts that are formed at different times, i.e., crustal recycling is independent of formation age. The evolution of $m(t,\tau)$ with such age-independent recycling may be expressed as:

$$\frac{\partial m(t,\tau)}{\partial t} = K_{mc}(t)\delta(t-\tau) - \frac{K_{rc}(t)}{M_{CC}(t)}m(t,\tau), \qquad (8)$$

where $\delta(t)$ is the Dirac delta function. The present-day cumulative formation age distribution, $CFD(\tau)$, may then be calculated as:

$$CFD(\tau) = \frac{1}{M_{CC}(t_p)}\int_0^\tau m(t_p,\tau')d\tau'. \quad (9)$$

Second, we model the cumulative surface age distribution (*CSD*) considering the combined effects of crustal generation, recycling, and reworking to the surface age distribution $s(t,\tau)$ of continental crust. Crustal reworking resets the apparent age of older crust, and since we consider the continental crust as a single reservoir, reworking uniformly affects older crust. That is, the surface age distribution, $s(t,\tau)$, may be calculated as:

$$\frac{\partial s(t,\tau)}{\partial t} = K_{mc}(t)\delta(t-\tau) - \frac{K_{rc}(t)}{M_{CC}(t)}s(t,\tau) + K_{rw}(t)\delta(t-\tau)$$

$$- \frac{K_{rw}(t)}{M_{CC}(t)}s(t,\tau)\big(1-\delta(t-\tau)\big). \quad (10)$$

The present-day cumulative surface age distribution, $CSD(\tau)$, may then be calculated as the present-day surface age distribution integrated over τ:

$$CSD(\tau) = \frac{1}{M_{CC}(t_p)} \int_0^{\tau} s(t_p, \tau') d\tau'. \quad (11)$$

Thermal evolution

The thermal evolution of Earth constrains the mantle processing rates to generate oceanic crust, K_{mo}, and hotspot islands, K_{mp}. First, we calculate K_{mo} considering that the oceanic crust is generated through decompressional melting beneath mid-ocean ridges, so its production rate can be directly linked with the thermal history of Earth. To be more concrete, the mantle processing rate for oceanic crust K_{mo} can be constrained based on plate velocity, V, and the initial depth of mantle melting, Z, as:

$$K_{mo}(t) = K_{mo}(t_p) \frac{Z(t)\, V(t)}{Z(t_p) V(t_p)}, \quad (12)$$

where $K_{mo}(t_p)$ is the present-day mantle processing rate at mid-ocean ridges, which is estimated to be 6.7x10^{14} kg/yr (*33*).

The initial depth of melting $Z(t)$ is controlled by mantle potential temperature, T_p, which can be calculated as (*32*):

$$Z(t) = \frac{T_p(t) - 1150}{g\rho_m(1.2 \text{ x } 10^{-7} - (\frac{dT}{dP})_S)}, \quad (13)$$

where g is gravitational acceleration (9.8 m/s^2), ρ_m is mantle density (3300 kg/m^3), and $(\frac{dT}{dP})_S$ is the adiabatic gradient in the mantle (1.54 x 10^{-8} K/Pa).

Then, using the relationship between surface heat flux and plate velocity, the temporal evolution of plate velocity can be calculated as:

$$V(t) = V(t_p)\left(\frac{Q(t)}{Q(t_p)}\frac{T_p(t_p)}{T_p(t)}\right)^2, \quad (14)$$

where the present-day plate velocity $V(t_p)$ is set to 5 cm/yr (*34*), and the present-day mantle heat flux $Q(t_p)$ is calculated as the difference between the present-day total terrestrial heat flux (46 ± 3 TW) (*35*) and the present-day continental crust heat production, $H_{cc}(t_p)$, as:

$$Q(t_p) = (46 + 3\varepsilon_1) - H_{CC}(t_p), \quad (15)$$

where ε_1 is a random variable, which can vary between -1 to 1.

The present-day continental crust heat production is considered to be (*24*):

$$H_{CC}(t_p) = 7.5 + 2.5\varepsilon_2 \quad (16)$$

where ε_2 is another random variable, whose range is between -1 to 1.

The evolution of mantle potential temperature, $T_p(t)$, can be tracked backward in time using the heat production, $H(t)$, the mantle heat flux, $Q(t)$, and the core heat flux, $Q_c(t)$, according to the following global energy balance (*31*):

$$C_m \frac{dT_p(t)}{dt} = H(t) - Q(t) + Q_c(t), \quad (17)$$

where C_m is the heat capacity of the whole mantle (4.97x10^{27} J/K).

In our model, we take the present-day core heat flux $Q_c(t_p)$ as a free parameter, which can vary from 5 to 15 TW. To track the evolution of core heat flux Q_c, we consider Q_c changes linearly with time:

$$Q_c(t) = \Delta Q_c(t_p - t)/t_p + Q_c(t_p), \quad (18)$$

where ΔQ_c is the difference between initial and present-day core heat flux, which can vary between 2 to 5 TW (*36*).

To integrate equation (17), we need to express H and Q as functions of time. Following Korenaga (*33*), H can be expressed as a function of time using the decay constants and heat production rates of major heat producing elements within Earth (^{238}U, ^{235}U, ^{232}Th, and ^{40}K) as following:

$$H(t) = H(t_p)\frac{\sum_{i=1}^{4} c_i p_i e^{\lambda_i t}}{\sum_{i=1}^{4} c_i p_i} \quad (19)$$

where c_i and p_i are the present-day relative concentration and the heat generation rate of the isotope in interest, λ_i are the decay constant, and $H(t_p)$ is the present-day mantle heat production, which is calculated as the total bulk silicate Earth heat production of 16 ± 3 TW (*37*) minus the present-day continental crust heat production $H_{cc}(t_p)$:

$$H(t_p) = (16 + 3\varepsilon_3) - H_{CC}(t_p) \quad (20)$$

where ε_3 is a random variable, whose range is between -1 to 1. Because the uncertainties of the terrestrial heat flux $Q(t_p)$, the present-day continental crust heat production $H_{cc}(t_p)$, and the present-day mantle heat production $H(t_p)$ are not related to each other, the three random variables, ε_1, ε_2, and ε_3 vary independently to each other.

As for the mantle heat flux Q, we assume it to be constant (36 TW) over the entire Earth history following Korenaga (*1*). This assumption results in mantle potential temperature T_p rising gradually from the present-day value of 1350 °C to approximately 1700 °C during Earth history. The classical scaling law, which can be expressed as $Q(t) \approx \alpha T_p(t)^{\beta}$, results in T_p quickly rises and reach to infinity, and such phenomenon is known as the thermal catastrophe. Compared with the classical scaling law, using a constant Q is more comparable with the evolution of the mantle potential temperature (e.g., *18*) as well as the geochemical model of Earth's composition. For more details of the two heat flux scaling laws, see Korenaga (*1, 33*). This validity of relatively constant heat flux becomes uncertain before ~3.5 Ga, as mantle potential temperature in such a deep time is not constrained observationally, and it is probably unrealistic to represent the thermal state of the very early Earth. However, the impact of this early phase of thermal evolution on argon degassing is limited thanks to our parameterization of mantle degassing rates (equation 5).

Knowing $Q_c(t)$, $Q(t)$, and $H(t)$, we can integrate equation (17) backward in time to obtain the mantle potential temperature $T_p(t)$ and then calculate the mantle processing rate to generate oceanic crust K_{mo} with equation (12).

Second, by assuming a linear relation between the mantle processing rate to generate hotspot islands K_{mp} and the core heat flux Q_c, we calculate K_{mp} as following:

$$K_{mp}(t) = K_{mp}(t_p)\frac{Q_c(t)}{Q_c(t_p)}, \quad (21)$$

where $K_{mp}(t_p)$ is the present-day rate of plume mass flux, which can be estimated from the present-day plume buoyancy flux, $f_{pb}(t_p)$, as:

$$K_{mp}(t_p) = \frac{f_{pb}(t_p)}{\alpha \Delta T}, \quad (22)$$

where $f_{pb}(t_p)$ is considered to be 55 x 10^3 kg/s (*38*), α is the thermal expansivity (4 x 10^{-5} K^{-1}), and ΔT is the temperature anomaly associated with mantle plumes (200 K).

The history of argon degassing

The different modes of degassing are considered before and after a sudden degassing event, which is assumed to have occurred in the early Earth (e.g., *14*). The high $^{40}Ar/^{36}Ar$ values (>10,000) reported for mantle-derived ultramafic rocks suggest a substantial degassing of primordial ^{36}Ar in the early Earth. Such catastrophic degassing is likely to have resulted from the highly energetic phase of planetary accretion. We denote the end of such an intense degassing phase by t_d. At t_d, the mantle loses a fraction of primordial argon, F_d, through sudden degassing to atmosphere, and after t_d, the mantle and the crust lose argon to the atmosphere in a gradual manner, corresponding to continuous crustal formation and destruction through Earth history. Since the detailed information of giant impacts is unknown, the timing of sudden degassing t_d and the degassing fraction F_d are both treated as free parameters in our model, with t_d varies from 0.05 Ga to 0.1 Ga and F_d from 10% to 80%, respectively.

From the beginning of the solar system, t_0, to the time of sudden degassing t_d, the parent isotope ^{40}K in the bulk silicate Earth (BSE) gradually decays through time, whereas the amount of daughter isotope ^{40}Ar in the BSE increases accordingly. Meanwhile, ^{40}Ar and ^{36}Ar in the BSE experience sudden degassing at t_d:

In the BSE domain:

$$\frac{d}{dt} N_{^{40}K}^{BSE}(t) = -\lambda N_{^{40}K}^{BSE}(t), \quad (23)$$

$$\frac{d}{dt} N_{^{40}Ar}^{BSE}(t) = \lambda_e N_{^{40}K}^{BSE}(t) - F_d \delta(t - t_d) N_{^{40}Ar}^{BSE}(t), \quad (24)$$

$$\frac{d}{dt} N_{^{36}Ar}^{BSE}(t) = -F_d \delta(t - t_d) N_{^{36}Ar}^{BSE}(t); \quad (25)$$

In the atmosphere domain (Atm):

$$\frac{d}{dt} N_{^{40}Ar}^{Atm}(t) = F_d \delta(t - t_d) N_{^{40}Ar}^{BSE}(t), \quad (26)$$

$$\frac{d}{dt} N_{^{36}Ar}^{Atm}(t) = F_d \delta(t - t_d) N_{^{36}Ar}^{BSE}(t), \quad (27)$$

where λ and λ_e are the total decay constant and branch decay constant of ^{40}K, respectively, and N is the number of atoms of the isotope denoted in the subscript contained in the reservoir denoted in the superscript. For example, the number of ^{40}K in the continental crust (CC) is denoted by $N_{^{40}K}^{CC}(t)$, which can also be expressed as:

$$N_{^{40}K}^{CC}(t) = \frac{C_{^{40}K}^{CC}(t) M_{cc}(t)}{m_{^{40}K}}, \quad (28)$$

where C is the concentration, M is the reservoir mass, and m is the atomic mass of the isotope in interest.

From t_d to the present day t_p, argon degassing is modeled as follows. The amount of ^{40}K in the continental crust is tracked backward in time according to its present-day abundance, and then scaled to be proportional to the growth of continental crust. The abundance of ^{40}K in the mantle is calculated from mass balance among the bulk silicate Earth, the mantle, and the continental crust. Argon degassing is considered to take place during mantle magmatism as well as crustal recycling and reworking, with the former parameterized by the mantle processing rates to generate continental crust K_{mc}, oceanic crust K_{mo}, and hotspot islands K_{mp}; and the latter by the crustal recycling rate K_{rc} and the reworking rate K_{rw}:

In the BSE domain:

$$\frac{d}{dt} N^{BSE}_{^{40}K}(t) = -\,\lambda\, N^{BSE}_{^{40}K}(t); \quad (29)$$

In the continental crust domain (CC):

$$N^{cc}_{^{40}K}(t) = N^{cc}_{^{40}K}(t_p) e^{\lambda t} \frac{M_{cc}(t)}{M_{cc}(t_p)}, \quad (30)$$

$$\frac{d}{dt} N^{CC}_{^{40}Ar}(t) = \lambda_e N^{CC}_{^{40}K}(t) - [K_{rw}(t) + K_{rc}(t)] N^{CC}_{^{40}Ar}(t), \quad (31)$$

$$\frac{d}{dt} N^{CC}_{^{36}Ar}(t) = -\,[K_{rw}(t) + K_{rc}(t)] N^{CC}_{^{36}Ar}(t); \quad (32)$$

In the mantle domain (M):

$$N^{M}_{^{40}K}(t) = N^{BSE}_{^{40}K}(t) - N^{CC}_{^{40}K}(t), \quad (33)$$

$$\frac{d}{dt} N^{M}_{^{40}Ar}(t) = \lambda_e N^{M}_{^{40}K}(t) - K_m(t) N^{M}_{^{40}Ar}(t), \quad (34)$$

$$\frac{d}{dt} N^{M}_{^{36}Ar}(t) = -\,K_m(t) N^{M}_{^{36}Ar}(t); \quad (35)$$

In the atmosphere domain:

$$\frac{d}{dt} N^{Atm}_{^{40}Ar}(t) = K_m(t) N^{M}_{^{40}Ar}(t) + [K_{rw}(t) + K_{rc}(t)] N^{CC}_{^{40}Ar}(t), \quad (36)$$

$$\frac{d}{dt} N^{M}_{^{36}Ar}(t) = K_m(t) N^{M}_{^{36}Ar}(t) + [K_{rw}(t) + K_{rc}(t)] N^{CC}_{^{36}Ar}(t), \quad (37)$$

where K_m is the combination of K_{mc} and the effective parts of K_{mo} and K_{mp}. Given that argon may not degas completely from basalts erupted in deep water, we consider the possibility of incomplete degassing at mid-ocean ridges (*39*). We also allow incomplete degassing for hotspot magmatism for three reasons: (1) the plume buoyancy flux estimate of Sleep (*38*) is subject to large uncertainties (*40*); (2) flux estimates based on swell topography are likely to be the upper bound of the buoyancy flux (*41*); and (3) thick lithosphere may hinder some of plume magma to reach the surface. The effective parts of K_{mo} and K_{mp} are modeled by free parameters $f^{K_{mo}}_{eff}$ and $f^{K_{mp}}_{eff}$, which can vary from 50% to 100% and 10% to 100%, respectively. We assume 100% efficiency during all of other degassing processes. The total mantle degassing rate K_m is calculated as follows:

$$K_m(t) = K_{mc}(t) + K_{mp}(t)\, f^{K_{mp}}_{eff} + K_{mo}(t)\, f^{K_{mo}}_{eff}. \quad (38)$$

In the above mass transfer equations, the five mass transfer rates K_{mo}, K_{mc}, K_{mp}, K_{rc}, and K_{rw} are the critical unknowns in our model. Constraining them with crustal growth and thermal evolution assures us to conduct the model in a self-consistent manner.

References and Notes

1. J. Korenaga, Initiation and evolution of plate tectonics on Earth: theories and observations. *Annu. Rev. Earth Planet. Sci.* **41**, 117-151 (2013).
2. M. Pujol, B. Marty, R. Burgess, G. Turner, P. Philippot, Argon isotopic composition of Archaean atmosphere probes early Earth geodynamics. *Nature* **498**, 87 (2013).
3. S. R. Taylor, S. M. McLennan, *The Continental Crust: Its Composition and Evolution* (Blackwell, Oxford, 1985).
4. R. L. Armstrong, Radiogenic isotopes: the case for crustal recycling on a near-steady-state no-continent-growth Earth, *Phil. Tram. R. Soc. Lond. A* **301**, 443-472 (1981).
5. B. K. Nelson, D. J. DePaolo, Rapid production of continental crust 1.7 to 1.9 by ago: Nd isotopic evidence from the basement of the North American mid-continent. *Geol. Soc. Am. Bull.* **96**, 746-754 (1985).
6. M. T. McCulloch, V. C. Bennett, Progressive growth of the Earth's continental crust and depleted mantle: geochemical constraints. *Geochim. Cosmochim. Acta* **58**, 4717-4738 (1994).
7. I. H. Campbell, Constraints on continental growth models from Nb/U ratios in the 3.5 Ga Barberton and other Archaean basalt-komatiite suites. *Am. J. Sci.* **303**, 319-351 (2003).
8. J. C. Rosas, J. Korenaga, Rapid crustal growth and efficient crustal recycling in the early Earth: Implications for Hadean and Archean geodynamics. *Earth Planet. Sci. Lett.* **494,** 42-49 (2018).
9. J. Korenaga, Crustal evolution and mantle dynamics through Earth history. *Philos. Trans. Royal Soc. A* **376**, 20170408 (2018).

10. K. C. Condie, R. C. Aster, Episodic zircon age spectra of orogenic granitoids: the supercontinent connection and continental growth. *Precambrian Res.* **180**, 227-236 (2010).

11. J. Korenaga, Estimating the formation age distribution of continental crust by unmixing zircon ages. *Earth Planet. Sci. Lett.* **482**, 388-395 (2018).

12. S. M. McLennan, S. R. Taylor, Geochemical constraints on the growth of the continental crust. *J. Geol.* **90**, 347-361 (1982).

13. D. R. Hilton, D. Porcelli, "Noble gases as mantle tracers" in *Treatise on Geochemistry* **Vol. 2**, Eds H. D. Holland, K. K. Turekian (2004), pp. 277–318.

14. Y. Hamano, M. Ozima, Earth-atmosphere evolution model based on Ar isotopic data. *Adv. Earth Planetary Sci.* **3**, 155-171 (1978).

15. M. Barboni, P. Boehnke, B. Keller, I. E. Kohl, B. Schoene, E. D. Young, K. D. McKeegan, Early formation of the Moon 4.51 billion years ago. *Sci. Adv.* **3**, e1602365 (2017).

16. J. Y. Lee, K. Marti, J. P. Severinghaus, K. Kawamura, H. S. Yoo, J. B. Lee, J. S. Kim, A redetermination of the isotopic abundances of atmospheric Ar. *Geochim. Cosmochim. Acta* **70**, 4507-4512 (2006).

17. N. M. W. Roberts, C. J. Spencer, The zircon archive of continent formation through time. *Geol. Soc.* **389**, 197-225 (2015).

18. C. Herzberg, K. Condie, J. Korenaga, Thermal history of the Earth and its petrological expression. *Earth Planet. Sci. Lett.* **292**, 79-88 (2010).

19. M. L. Bender, B. Barnett, G. Dreyfus, J . Jouzel, D. Porcelli, The contemporary degassing rate of 40Ar from the solid Earth. *Proc. Natl. Acad. Sci. U.S.A.* **105**, 8232-8237 (2008).

20. T. M. Harrison, The Hadean crust: evidence from > 4 Ga zircons. *Annu. Rev. Earth Planet. Sci.* **37**, 479-505 (2009).
21. M. Tang, K. Chen, R. L. Rudnick, Archean upper crust transition from mafic to felsic marks the onset of plate tectonics. *Science* **351**, 372-375 (2016).
22. C. B. Keller, B. Schoene, Statistical geochemistry reveals disruption in secular lithospheric evolution about 2.5 Gyr ago. *Nature* **485**, 490-493 (2012).
23. K. C. Condie, Chemical composition and evolution of the upper continental crust: contrasting results from surface samples and shales. *Chem. Geol.* **104**, 1-37 (1993).
24. Rudnick, R. L., Gao, S., "Composition of the Continental Crust" in *Treatise on Geochemistry* **Vol. 3**, Eds H. D. Holland, K. K. Turekian (Pergamon, 2003), pp. 1–64.
25. R. Parai, S. Mukhopadhyay, Xenon isotopic constraints on the history of volatile recycling into the mantle. *Nature* **560**, 223-227 (2018).
26. A. V. Sobolev, E. V. Asafov, A. A. Gurenko, N. T. Arndt, V. G. Batanova, M. V. Portnyagin, D. Garbe-Schönberg, A. H. Wilson, G. R. Byerly, Deep hydrous mantle reservoir provides evidence for crustal recycling before 3.3 billion years ago. *Nature* **571**, 555-559 (2019).
27. B. Marty, D. V. Bekaert, M. W. Broadley, C. Jaupart, Geochemical evidence for high volatile fluxes from the mantle at the end of the Archaean. *Nature* **575**, 485-488 (2019).
28. R. L. Armstrong, Comment on "Crustal growth and mantle evolution: inferences from models of element transport and Nd and Sr isotopes." *Geochim. Cosmochim. Acta* **45**, 1251 (1981).
29. M. D. Hopkins, T. M. Harrison, C. E. Manning, Constraints on Hadean geodynamics from mineral inclusions in > 4 Ga zircons. *Earth Planet. Sci. Lett.* **298**, 367-376 (2010).

30. J. Korenaga, N. J. Planavsky, D. A. Evans, Global water cycle and the coevolution of the Earth's interior and surface environment. *Philos. Trans. Royal Soc. A 375*, 20150393(2017).

31. J. Korenaga, Pitfalls in modeling mantle convection with internal heat production. *J. Geophys. Res. Solid Earth* **122**, 4064-4085 (2017).

32. C. M. Padhi, J. Korenaga, M. Ozima, Thermal evolution of Earth with xenon degassing: A self-consistent approach. *Earth Planet. Sci. Lett.* **341**, 1-9 (2012).

33. J. Korenaga, Archean geodynamics and the thermal evolution of Earth. *Geophysical Monograph-American Geophysical Union* **164**, 7 (2006).

34. B. Parsons, The rates of plate creation and consumption. *Geophys. J. Int.* **67**, 437-448 (1981).

35. C. Jaupart, S. Labrosse, J. C. Mareschal, "Temperatures, heat and energy in the mantle of the Earth" in *Treatise on Geophysics Vol. 7,* Eds G. Schubert (Elsevier, 2007), pp. 253-303.

36. J. G. O'Rourke, J. Korenaga, D. J. Stevenson, Thermal evolution of Earth with magnesium precipitation in the core. *Earth Planet. Sci. Lett.* **458**, 263-272 (2017).

37. T. Lyubetskaya, J. Korenaga, Chemical composition of Earth's primitive mantle and its variance: 2. Implications for global geodynamics. *J. Geophys. Res. Solid Earth* **112**, B03212 (2007).

38. N. H. Sleep, Hotspots and mantle plumes: Some phenomenology. *J. Geophys. Res. Solid Earth* **95**, 6715-6736 (1990).

39. P. Sarda, D. Graham, Mid-ocean ridge popping rocks: implications for degassing at ridge crests. *Earth Planet. Sci. Lett.* **97**, 268-289 (1990).

40. S.D. King, C. Adam, Hotspot swells revisited. *Phys. Earth Planet. Inter.* **235**, 66-83 (2014).

41. J. Korenaga, Firm mantle plumes and the nature of the core–mantle boundary region. *Earth Planet. Sci. Lett.* **232**, 29-37 (2005).

Acknowledgements

This article was based on work supported by National Science Foundation under grant EAR-1753916. The authors thank three anonymous reviewers for constructive comments and suggestions.

Competing Interests: The authors declare that they have no competing interests.

Author Contributions: M. G. performed the modeling and wrote the manuscript. J. K. designed the project, discussed the results, and commented on the manuscript.

Data and materials availability: All data needed to evaluate the conclusions in the paper are present in the paper and/or the Supplementary Materials. MATLAB scripts used for our modeling are also included in the Supplementary Materials.

Figures and Tables

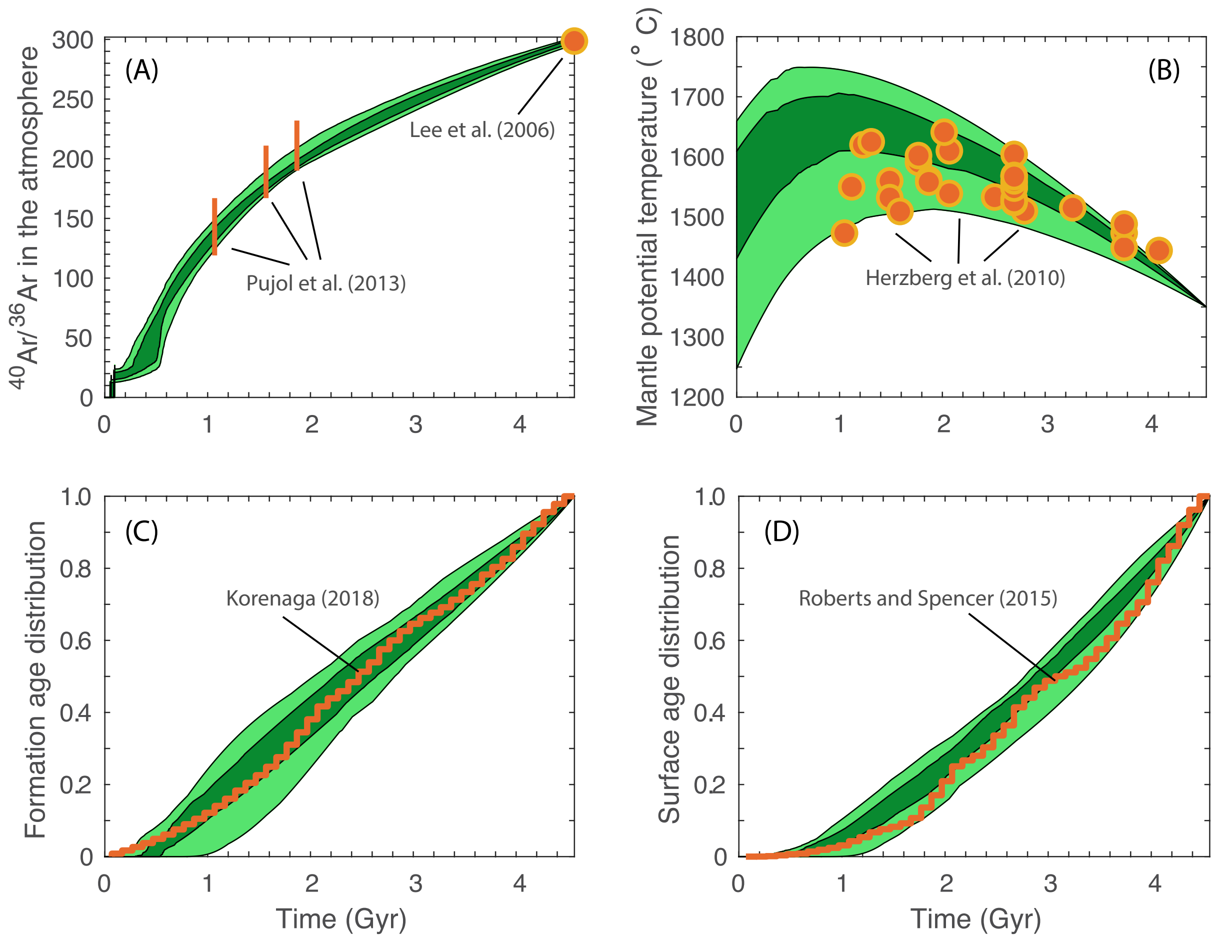

Fig. 1. Observational constraints and the distribution of successful model solutions. Observational constraints used to select successful solutions are shown in orange. The 50th and 90th percentiles of successful solutions are shown in dark green and light green, respectively. (A) $^{40}Ar/^{36}Ar$ in the atmosphere. Orange bars are based on $^{40}Ar/^{36}Ar$ measurements of Archean hydrothermal quartz by Pujol et al. (*2*), and orange dot is the present-day $^{40}Ar/^{36}Ar$ from Lee et al. (*16*). (B) Mantle potential temperature. Oranges dots are the Archean and Proterozoic mantle potential temperatures from Herzberg et al. (*18*). (C) Present-day cumulative distribution of crustal formation age. Orange line is from Korenaga (*11*). (D) The present-day cumulative distribution of crustal surface age. Orange line is based on the distribution of zircon U-Th crystallization ages (*17*).

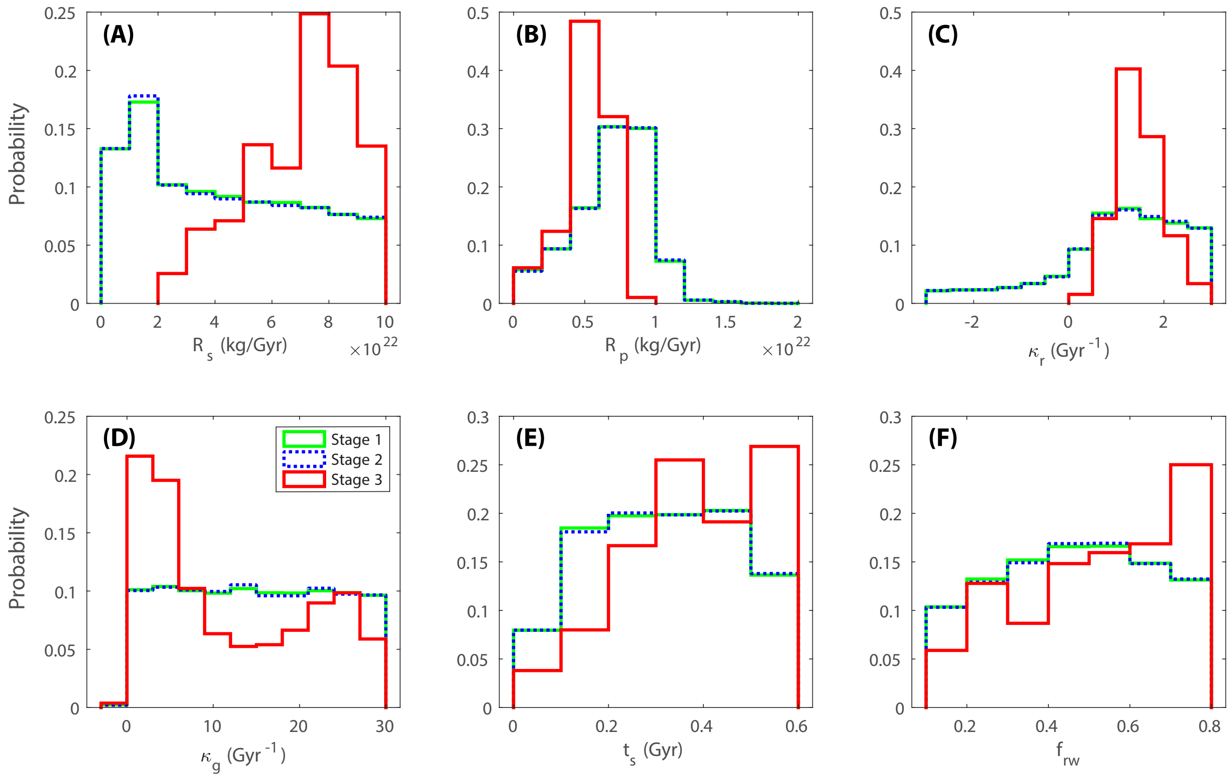

Fig. 2. The a posteriori distributions of crustal evolution parameters, based on ~2x10^4, ~2.5x10^4, and ~3x10^3 successful Monte Carlo solutions from stage 1, 2, and 3, respectively. Distributions from stage 1, 2, and 3 are shown in green, blue, and red, respectively. (A) Initial recycling rate, (B) present-day recycling rate, (C) decay constant for crustal recycling, (D) decay constant for crustal generation, (E) onset time for crustal formation, and (F) reworking factor.

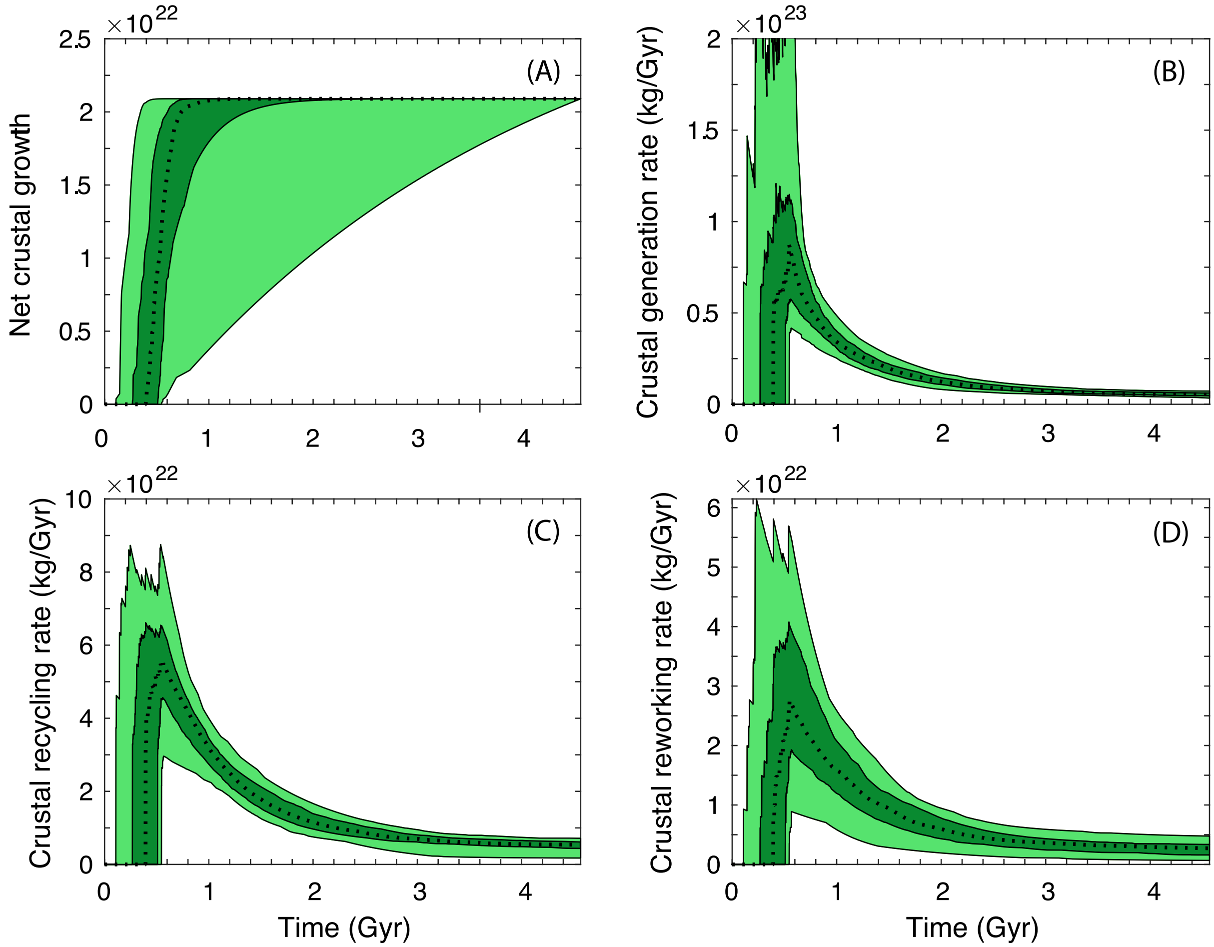

Fig. 3. Net crustal growth and crustal generation and destruction rates, based on ~3x10^3 successful Monte Carlo solutions. The middle 50 % and 90 % of our successful solutions are shown in dark green and light green, respectively. The medians of the successful solutions are shown in black dotted lines. (A) Net crust growth, (B) crustal generation rate, (C) crustal recycling rate, and (D) crustal reworking rate.

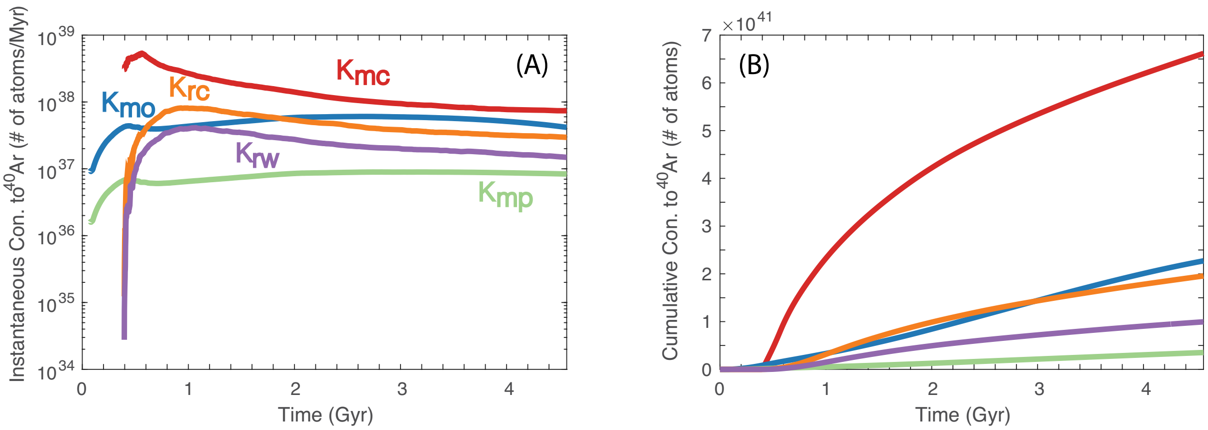

Fig. 4. Instantaneous and cumulative contributions of individual mass transfer rates to atmospheric ^{40}Ar, based on the medians of ~3x10^{3} successful Monte Carlo solutions. Mantle processing rates to generate continental crust (K_{mc}), oceanic crust (K_{mo}), hotspot islands (K_{mp}) are shown in red, dark blue, and green, respectively. Crustal recycling (K_{rc}) and reworking (K_{rw}) rates are shown in yellow and light blue, respectively. (A) Instantaneous contributions and (B) cumulative contributions of individual mass transfer rates to atmospheric ^{40}Ar.

Table 1. List of independent variables in argon degassing model.

Parameter	Definition	Value	Unit
t_d	Timing of sudden degassing	0.05 to 0.1	Gyr
F_d	Sudden degassing fraction	10 % to 80 %	-
$^{36}Ar(t_0)$	Initial amount of ^{36}Ar in bulk silicate Earth	2 x 10^{39} to 2 x 10^{40}	# of atoms
κ_r	Decay constant of crustal recycling rate	-3 to 3	Gyr^{-1}
κ_g	Decay constant of crustal generation rate	-1 to 30	Gyr^{-1}
R_s	Initial crustal recycling rate	0 to 10 x 10^{22}	kg Gyr^{-1}
R_p	Present-day crustal recycling rate	0 to 2 x 10^{22}	kg Gyr^{-1}
t_s	Crustal growth starting point	0.057 to 0.567	Gyr
f_{rw}	Crustal reworking rate factor	0.1 to 0.8	-
$H_{BSE}(t_p)$	Present-day BSE heat production	13 to 19	TW
$H_{CC}(t_p)$	Present-day continental crust heat production	5 to 10	TW
$Q_{total}(t_p)$	Present-day total terrestrial heat flux	43 to 49	TW
$Q_c(t_p)$	Present-day core heat flux	5 to 15	TW
ΔQ_c	Difference between initial and present-day Q_c	2 to 5	TW
$f_{eff}^{K_{mo}}$	Incomplete degassing factor for mid-ocean ridge degassing	50 % to 100 %	-
$f_{eff}^{K_{mp}}$	Incomplete degassing factor for mantle plume degassing	10 % to 100 %	-

Table 2. List of dependent variables in argon degassing model.

Parameter	Definition	Calculation
$Q(t_p)$	Present-day mantle heat flux	$Q(t_p) = Q_{total}(t_p) - H_{CC}(t_p)$
$^{40}K_{BSE}(t_p)$	Present-day ^{40}K in the BSE	Calculate according to $H_{BSE}(t_p)$
$^{40}K_{cc}(t_p)$	Present-day ^{40}K in the continental crust	Calculate according to $H_{CC}(t_p)$
Q_c	Core heat flux	$Q_c(t) = \Delta Q_c(t_p - t)/t_p + Q_c(t_p)$
K_{mp}	Hotspot islands generation rate	$K_{mp}(t) = K_{mp}(t_p)\frac{Q_c(t)}{Q_c(t_p)} f_{eff}^{K_{mp}}$
K_{mo}	Oceanic crust generation rate	$K_{mo}(t) = K_{mo}(t_p)\frac{Z(t)\,V(t)}{Z(t_p)V(t_p)} f_{eff}^{K_{mo}}$

List of Supplementary materials:

Materials and Methods

Fig S1. The a posteriori distributions of independent model parameters, based on ~2.5×10^4 and ~3×10^3 successful Monte Carlo solutions from stage 2 and 3, respectively.

Data S1. Data in Fig.1-4 and Fig.S1

Data S2. Input data for the argon degassing code